DALTON
FULL PAPER

A new chiral metalladiphosphine for early–late chemistry. Crystal structure of a D-camphor-based zirconium enolato phosphine and rearrangement of heterobimetallic Zr/Pd complexes†

Chris Mattheis,[a] Pierre Braunstein *[a] and Axel Fischer[b]

[a] *Laboratoire de Chimie de Coordination, UMR 7513 CNRS, Université Louis Pasteur, 4 rue Blaise Pascal, 67070 Strasbourg Cedex, France. E-mail: braunst@chimie.u-strasbg.fr*

[b] *Chemisches Institut, Otto-von-Guericke-Universität Magdeburg, Universitätsplatz 2, Gebäude 16, 39106 Magdeburg, Germany*

Received 12th October 2000, Accepted 22nd January 2001
First published as an Advance Article on the web 26th February 2001

The bis(phosphinoenolato) zirconocene **2**, prepared from the phosphino camphor derivative 3-*exo*-$\mathrm{PPh_2C_{10}H_{15}O}$ **1**, represents the first C_2-symmetric chiral diphosphine containing an early transition metal centre tethered to the phosphino groups *via* an enolato linkage. It allows the selective assembly of Lewis-acid early–late bimetallic combinations, as exemplified with the Zr/Cu and Zr/Ag complexes **4** and **5**. The monophosphinoenolato titanocene **3** was also prepared. Reactions of **2** or **3** with $[\mathrm{Pd(dmba)}(\mu\text{-}\mathrm{Cl})]_2$ (dmba = *o*-$\mathrm{C_6H_4CH_2NMe_2}$) or $[\mathrm{PdCl_2(SEt_2)_2}]$ led to complete transfer of the functional ligand to the Pd(II) centre, with formation of $[(\mathrm{dmba})\overline{\mathrm{Pd}(\mathrm{PPh_2C_{10}H_{14}O}})]$ **6** or *cis*-$[\overline{\mathrm{Pd}(\mathrm{PPh_2C_{10}H_{14}O}})_2]$ **8** and $[\mathrm{Cp_2ZrCl_2}]/[\mathrm{Cp_2TiCl_2}]$, respectively. A heterobimetallic Zr/Pd intermediate complex **10** of this rearrangement could be detected. Complexes **6** and **8** were prepared independently by reaction of **1** with $[\mathrm{Pd(dmba)}(\mu\text{-}\mathrm{Cl})]_2$ or $[\mathrm{Pd(SEt_2)_2Cl_2}]$, respectively, which first afforded complexes **7** and **9** which were then treated with KH. The crystal structures of **2**, **6** and **8**·THF·$\mathrm{H_2O}$ have been determined by X-ray diffraction.

Introduction

Two particularly active research areas in inorganic and organometallic chemistry concern chiral diphosphine ligands owing to their applications in homogeneous catalysis,[1–3] and the study of metal complexes with phosphorus–oxygen hybrid ligands whose hard/soft character allows hemilabile behaviour in solution[4] or confers unique catalytic properties.[5] With the desire of combining these two facets of metal–phosphine chemistry, we prepared a new chiral diphosphine consisting of two enolato phosphine ligands oxygen-bonded to a zirconocene unit. This unique early metal centred ligand system should subsequently allow the synthesis of early–late heterobimetallic complexes. Combining two metals with contrasting properties in the same molecule not only offers the potential of inducing novel chemical transformations that would not be possible with either metal alone but may also improve the yield or selectivity of existing reactions.[6]

Results and discussion

Slight modifications of the literature method enabled us to increase the yield of the D-camphor-based β-keto phosphine (1*R*)-*endo*-(+)-3-diphenylphosphino-1,7,7-trimethylnorborn-2-one **1** from 37%[7] to 65% (see Experimental section). Reactions of **1** with $[\mathrm{Cp_2ZrCl_2}]$ and $\mathrm{NEt_3}$, or with $[\mathrm{Cp_2ZrMe_2}]$ were unsuccessful; however treatment of **1** with *n*-BuLi at −78 °C followed by the addition of $[\mathrm{Cp_2ZrCl_2}]$ in a 2 : 1 stoichiometry led to the formation of the colourless zirconocene complex **2** in 70% yield (Scheme 1).

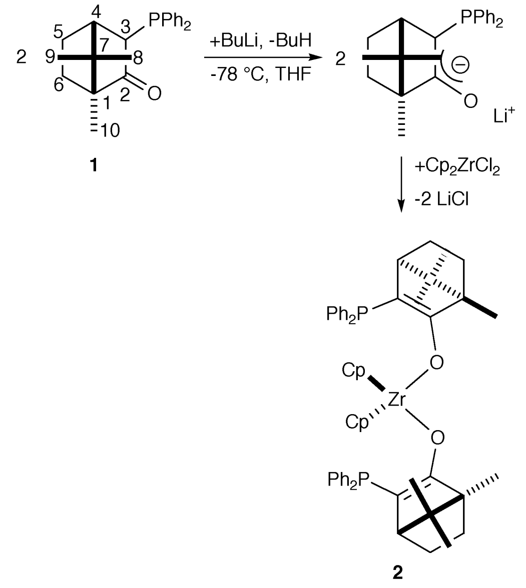

Scheme 1

This highly moisture-sensitive complex was characterized by NMR spectroscopy and X-ray diffraction (see Experimental section). The presence of the basic P atoms within the molecule may enhance the sensitivity of the Zr–O bond to water, the splitting of $\mathrm{H_2O}$ to hydroxy ions and protons being triggered by formation of phosphonium ions. The $^{31}\mathrm{P}\{^1\mathrm{H}\}$ NMR resonance for compound **2** at δ −31.8 is shifted to higher field compared to that of the free ligand **1** (δ 0.1 for **1**), owing to the formation of the enolate species. Similarly, the $^{13}\mathrm{C}$ NMR resonance of C(2) (δ 184.44) is shifted to higher field compared to **1** (δ 218.2, d, $^2J_{\mathrm{PC}} = 7.3$ Hz in **1**[7]), whereas a downfield shift is observed for C(3) (δ 100.24) and H(4) (δ 2.4) [for **1**: δ C(3) = 54.2, d, $^1J_{\mathrm{PC}} = 28.4$ Hz;[7] ^{1}H NMR: δ H(4) = 1.93]. Interestingly, the carbon atoms of the Cp ligands show coupling to phosphorus.[8]

---

† Dedicated to Professor H. Schnöckel on the occasion of his 60th birthday, with our most sincere congratulations.

DOI: 10.1039/b008227i

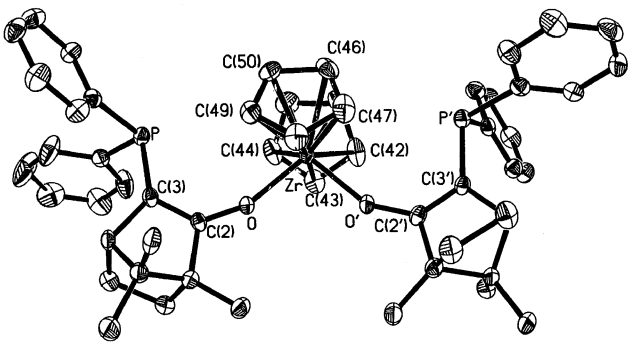

Fig. 1 An ORTEP view of the structure of **2**. Thermal ellipsoids are drawn at the 30% probability level.

Single crystals of **2**, suitable for X-ray analysis, were grown from toluene–*n*-hexane. The ligand arrangement around the metal is pseudo-tetrahedral (Fig. 1) and it is noteworthy that the bulky enolato phosphine ligands are wrapped back towards the Zr atom. The O–Zr–O′ plane bisects the Cp–Zr–Cp (Cp = midpoint of cyclopentadienyl ring) angle of 50.8° [Cp(C41–C45)–(O–Zr–O′)] 25.5°; (O–Zr–O′)–Cp(C46–C50) 25.3°. The ligand conformations within the two slightly different best planes defined by P–C(3)–C(2)–O and P′–C(3′)–C(2′)–O′, respectively, may result from packing effects. A related situation has been observed with the enolate ligands in $[Cp_2Ti(OCH{=}CH_2)_2]$.[9] The rather short Zr–O distances [2.002(4) Å av.] and the large Zr–O–C bond angles [154.0(3) av.] indicate some metal–oxygen π interactions.[10,11] The C–O bond distances [1.330(6) Å av.] are typical for a C_{sp^2}–O single bond (statistical average 1.34 Å) and together with the value of the C(2)–C(3) bond length [1.361(6) Å av.], this indicates a reduced electron delocalization within the enolato moiety.[11,12]

A careful choice of the metal is crucial for the formation of a metal centred diphosphine ligand. Thus, reaction of two equivalents of lithiated **1** with $[Cp_2TiCl_2]$ led to a mixture of titanium enolato phosphine species with partial loss of the Cp moieties. This stands in contrast to the synthesis of the bisenolato complexes $[Cp_2Ti(OCH{=}CH_2)_2]$[9] or $[Cp_2Ti(OCMe{=}CH_2)_2]$[10a] and may be due to increased steric hindrance in our case. Accordingly, the use of only one equivalent of lithiated **1** afforded the monoenolato phosphine titanium complex **3** in 70% yield which was characterized by NMR spectroscopy (see Experimental section).

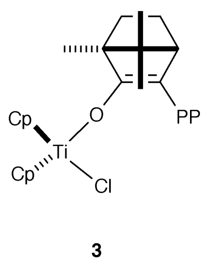

3

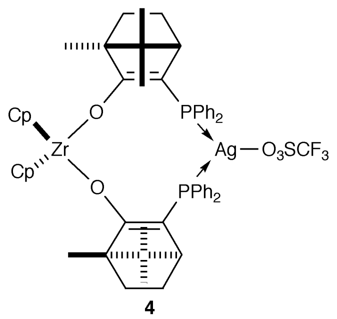

4

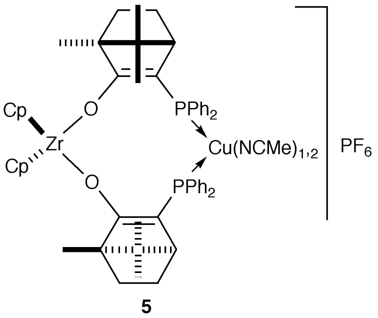

5

Preliminary complexation studies with late transition metals have shown that **2** is indeed able to behave as a chelating metalladiphosphine. Rotation of the camphor moiety about the Zr–O bond allows **2** to react with silver(I) triflate or $[Cu(NCMe)_4]PF_6$ hexafluorophosphate to form the new chiral heterobimetallic early–late transition metal complexes **4** and **5** with Lewis-acid properties. They were too sensitive to give satisfactory elemental analysis but could be characterized by NMR spectroscopy and mass spectrometry (see Experimental section).

However, no heterobimetallic Zr/Pd or Ti/Pd complexes could be isolated when **2** or **3** were reacted with $[Pd(dmba)(\mu\text{-}Cl)]_2$ (dmba = $o\text{-}C_6H_4CH_2NMe_2$). Instead, $[Cp_2ZrCl_2]$ or $[Cp_2TiCl_2]$ were detected in the ^{1}H NMR spectrum and the singlet at δ 26.8 in the ^{31}P NMR spectrum of the reaction mixture was assigned to the palladium phosphino enolate complex **6** [eqn. (1)].

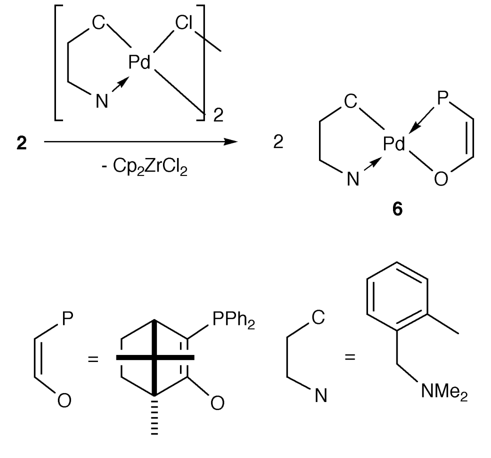

(1)

Similarly, reactions with the chloride-free, cationic complex $[Pd(dmba)(NCMe)_2]PF_6$ only allowed identification of **6** among the products.

Complex **6** was prepared independently by reaction of **7** (see below), obtained from **1** and $[Pd(dmba)(\mu\text{-}Cl)]_2$ (Scheme 2), with KH. It is sensitive to hydrolysis.

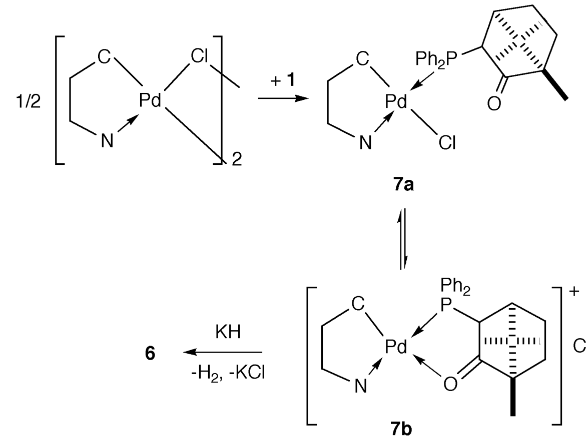

Scheme 2

Crystals of **6** suitable for X-ray determination were obtained from dichloromethane–*n*-hexane. The coordination geometry around the metal is square planar (Fig. 2). The palladium is chelated by the dmba moiety and coordination of the phosphorus occurs in *cis* position to the aryl group, in agreement with the antisymbiotic effect[13] and with other related structures.[14] The coordination sphere of the palladium atom is completed by the oxygen atom of the phosphinoenolate ligand. The Pd–O and Pd–P bond distances in **6** [2.122(6) and 2.254(3) Å,

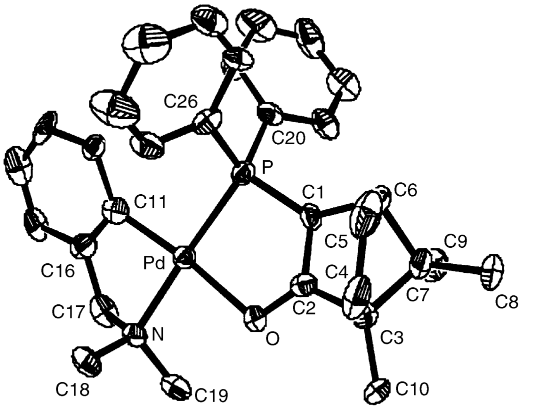

Fig. 2 An ORTEP view of the structure of **6**. Thermal ellipsoids are drawn at the 30% probability level.

respectively] are slightly longer than in the related complexes with a negatively charged oxygen donor atom [(dmba)Pd{$Ph_2PCH_2C(O)O$}],[14a] [(dmba)Pd{Ph_2PCH⋯C(⋯O)OEt}][14b] and [(dmba)Pd[Ph_2PC{C(O)NHPh}C(Ph)O],[14c] [2.105(3)/2.218(1), 2.117(5)/2.242(2) and 2.096(3)/2.234(1) Å, respectively]. The bond distances and angles around the dmba moiety and around the phosphorus atom all are in the expected range.

The air-stable complex **7** was obtained in 77% yield according to Scheme 2. Conductivity measurements proved it to be an 1 : 1 electrolyte with a molar conductivity of $\Lambda_m = 59\ \text{S cm}^2\ \text{mol}^{-1}$ in methanol, which is less than the expected value for a fully dissociated ion pair such as [(dmba)Pd($Ph_2PC_{10}H_{16}OH$)]Cl which contains a limonene-based phosphino-alcohol ligand ($\Lambda_m = 74\ \text{S cm}^2\ \text{mol}^{-1}$, dissociated to 100% in methanol).[15] We thus assume the existence of an equilibrium between a neutral (**7a**) and a cationic species (**7b**). In polar solvents (methanol) **7b** is stabilized by coordination of the keto group, a situation similar to that observed in other cationic β-ketophosphine palladium complexes with a five-membered ring chelate, such as [(dmba)Pd{$Ph_2PCH_2C(O)Ph$}](CF_3SO_3)[16a] and *cis*-[Pd{$Ph_2PCH_2C(O)Ph$}$_2$](BF_4)$_2$.[16b]

The reaction of **2** with [$PdCl_2(SEt_2)_2$] also led to a ligand exchange and resulted in the formation of the bis(phosphinoenolate) palladium complex *cis*-[Pd($Ph_2PC_{10}H_{14}O$)$_2$] **8** and [Cp_2ZrCl_2] (Scheme 3). Similar results were observed with the platinum precursor [$PtCl_2(NCPh)_2$]. Complex **8** was prepared independently by reaction of **1** with [$PdCl_2(SEt_2)_2$] (formation of **9**) followed by treatment with potassium hydride. Complexes **8** and **9** have been previously prepared by different routes.[7,17]

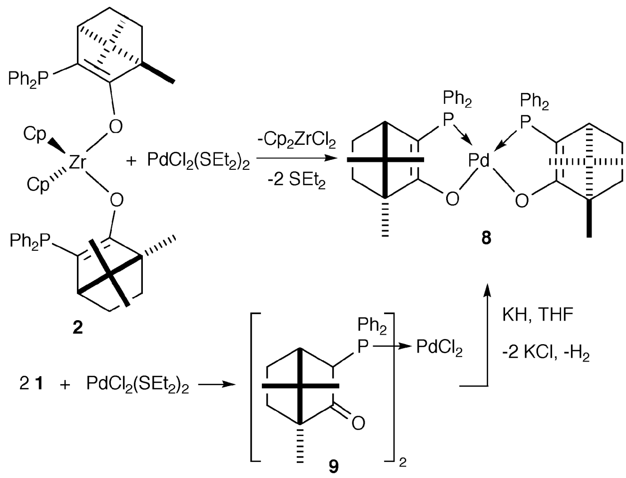

Scheme 3

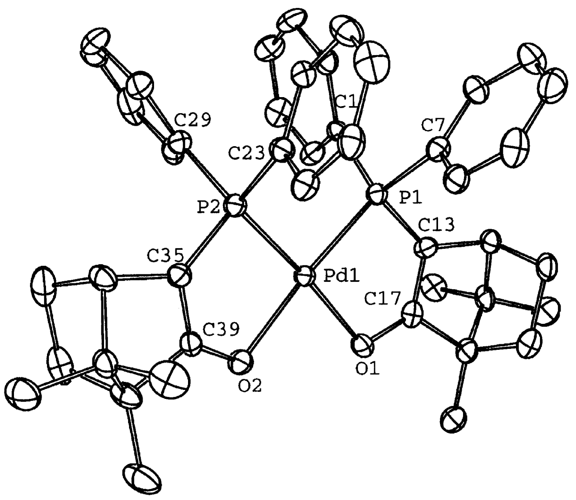

Fig. 3 An ORTEP view of the structure of **8** in **8**·THF·H_2O. Thermal ellipsoids are drawn at the 30% probability level.

Crystals of **8** suitable for X-ray determination were obtained from THF–*n*-hexane. The unit cell of **8** contains one molecule of water and of THF, which do not interact with the metal complex. We find the expected *cis*-arrangement of the chelating phosphinoenolate ligands around the square planar coordinated palladium (Fig. 3). The Pd–O bond distances [2.097(4) and 2.093(4) Å] are relatively short compared to the examples cited above (see discussion for **6**)[14a–c] whereas the Pd–P bond distances [2.260(2) and 2.254(2) Å] are somewhat longer.

For the rearrangement leading to the transfer of the phosphinoenolate ligand from Zr to Pd, we suggest the sequence shown in Scheme 4.

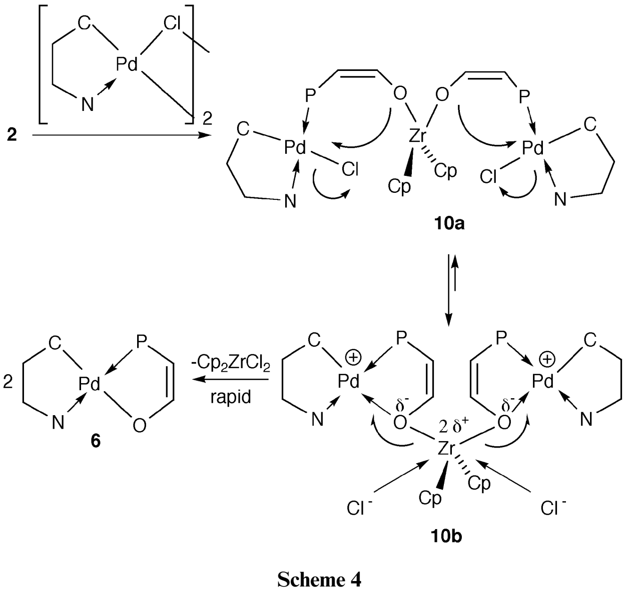

Scheme 4

Reaction of **2** with [Pd(dmba)(μ-Cl)]$_2$ should occur by a classical phosphine-induced chloride-bridge splitting reaction and yield the heterobimetallic complex **10** which is present in a neutral (**10a**) and a cationic complex (**10b**). In cationic **10b** the oxygen of the enolato function is coordinated to the palladium. This can be compared with the cationic structures of **7b**, [(dmba)Pd{$Ph_2PCH_2C(O)Ph$}](CF_3SO_3) and *cis*-[Pd{$Ph_2PCH_2C(O)Ph$}$_2$](BF_4)$_2$.[16] Complex **10b** contains already the structural components of the chelate complex **6**. Nucleophilic attack of the chlorides at the zirconium and switching the Zr–O electron pair to the palladium would lead to **6** and [Cp_2ZrCl_2]. If the equilibrium of the bimetallic species is shifted to **10b** but the latter rearranges much faster to **6** than reacts back to **10a**, it will not be possible to observe any Zr–Pd complex. Although this remains difficult to prove, we could provide at least partial evidence for this mechanism. By shifting the equilibrium with added salt, neutral **10a** could be stabilized enough to be analysed by NMR spectroscopy and mass spectrometry. In the presence of added LiBr a broad singlet was observed in the ^{31}P NMR spectrum at δ 25.25 which is close to that for **6** (δ 26.76) (**2** was always present in amounts less than 5%) and this is consistent with the very similar environments of the phosphorus atoms in **6** and **10a**. At −40 °C, the signals in the ^{31}P and ^{1}H NMR spectra become sharper. Two signals are observed in the ^{31}P NMR spectrum, the major one corresponds to **10a** whereas the smaller is assigned to the bromide analogue resulting from halide exchange. Adventitious hydrolysis of **10a** in an NMR tube led to the formation of **7a**,**b** and their bromide analogues (δ 36.5, 36.8) and [$(Cp_2ZrCl)_2O$]. In the mass spectrum, the peaks at *m*/*z* 832.0 and 575.1 were assigned to **A** and **6**, respectively, and could result from fragmentation of **10a**.

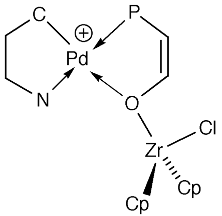

A

An alternative, stepwise mechanism (Scheme 5) may be envisaged which cannot be distinguished from that of Scheme 4 with the present data.

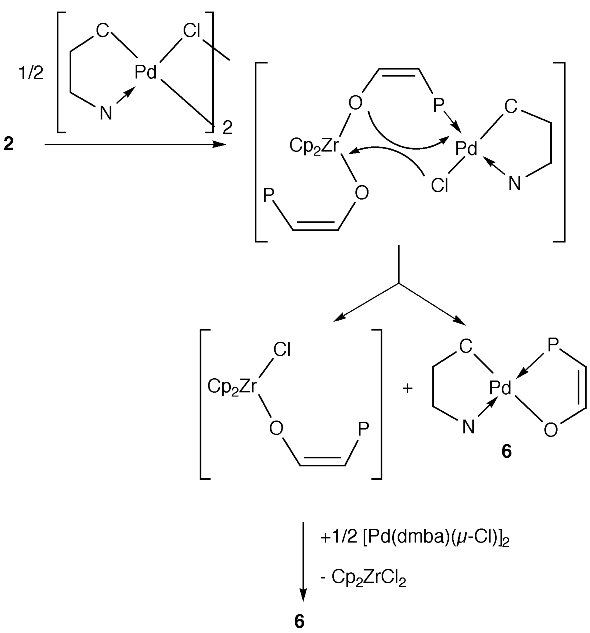

Scheme 5

Conclusion

By using the new bis(phosphinoenolato)zirconocene complex **2** we could access new chiral heterobimetallic Zr/Ag and Zr/Cu complexes. With Pd(II) precursors, a ligand redistribution reaction leading to [Cp_2ZrCl_2] and **6** was observed for which a neutral (**10a**) and a cationic (**10b**) Zr/Pd species are suggested intermediates. They exist in an equilibrium but only **10a** may be observed by shifting the equilibrium with LiBr, because **10b** rearranges by loss of [Cp_2ZrCl_2] to **6** faster than it reacts back to **10a**. The rearrangement is driven by the favourable formation of a chelate complex and by the nucleophilic attack of the chlorides at the zirconium leading to [Cp_2ZrCl_2]. If the tendency to form chelate complexes is reduced, heterobimetallic complexes can be obtained, as shown in the case of the Zr–Ag/Zr–Cu complexes **4** and **5**, respectively.

These results indicate that a careful choice of the second metal is necessary to observe a bridging mode for the *P*,*O*-ligand. Another promising approach to prepare stable phosphinoenolato heterobimetallic complexes consists of the tuning of the ligands, for instance by using aromatic ligands such as phenolates on the early transition metal (which would also lower the sensitivity of the complexes towards water). Finally, a reduced number of Cp ligands at the zirconium in **2** should lead to increased Lewis acidity of the metal.

Experimental

General procedures

All reactions and manipulations were carried out under an inert atmosphere of purified nitrogen using standard Schlenk-tube techniques. Nitrogen (Air liquide, R-grade) was passed through BASF R3-11 catalyst and 4 Å molecular sieve columns to remove residual oxygen and water. Solvents were dried and distilled under nitrogen before use: pentane, hexane and toluene over sodium, tetrahydrofuran and diethyl ether over sodium–benzophenone, acetonitrile and dichloromethane over calcium hydride. Elemental C, H and N analyses were performed by the Service de microanalyses du CNRS. The ^{1}H, ^{31}P{^{1}H} and ^{13}C{^{1}H} NMR spectra were recorded at 300.1, 121.5 and 75.5 MHz respectively, on a Bruker AM300 instrument. Phosphorus chemical shifts were externally referenced to 85% H_3PO_4 in H_2O with downfield chemical shifts reported as positive. All NMR spectra were run at room temperature in $CDCl_3$ if not stated otherwise. Conductivity measurements were carried out in methanol at room temperature. Electrospray mass spectra were run on a HP 1100 series LC/MSD spectrometer.

Preparations

Synthesis of 1. Reaction of one equivalent of (1*R*)-*endo*-(+)-3-bromocamphor in THF with 1.1 equivalent of *n*-BuLi at −78 °C was followed by the addition of 1 equivalent of PPh_2Cl at −78 °C. The mixture was stirred overnight and the solvent was removed under reduced pressure. Column chromatography on silica gel with Et_2O as the eluent afforded **1** in 65% yield as a white solid. Analytical data were in agreement with literature values.[7]

Synthesis of 2. Reaction of two equivalents of **1** in THF with 1.1 equivalent of *n*-BuLi at −78 °C was followed by the addition of 0.5 equivalent of [Cp_2ZrCl_2] at −78 °C. The mixture was stirred overnight and the solvent was removed under reduced pressure. Recrystallisation from toluene–*n*-hexane afforded **2** in 70% yield as a white solid. Satisfactory elemental analyses could not be obtained owing to the moisture sensitivity of the complex. ^{1}H NMR: δ 0.66 [m, 2H, H(5)], 0.74 (s, 6H, Me), 0.93 (s, 6H, Me), 1.11 (s, 6H, Me), 1.48 [m, 2H, H(6)], 1.20 [m, 2H, H(6′)], 1.62 [m, 2H, H(5′)], 2.4 [br, 2H, H(4)], 6.44 (s, 10H, Cp), 7.29–7.36/7.52–7.57 (2 m, 20H, Ph); ^{13}C NMR: δ 11.09 [s, C(10)], 20.09/20.84 [2 s, C(8/9)], 27.68 [s, C(5)], 32.55 [s, C(6)], 51.97 [d, $^{2}J_{PC} = 6.0$, C(4)], 53.94 [s, C(7)], 57.21 [d, $^{3}J_{PC} = 5.9$, C(1)], 100.24 [d, $^{1}J_{PC} = 9.5$, C(3)], 113.83 (t, $^{5}J_{PC} = 3.0$, Cp), 127.20 (s, *p*-Ph), 128.00 (s, *p*-Ph′), 128.02 (d, $^{3}J_{PC} = 3.7$, *m*-Ph), 128.16 (d, $^{3}J_{PC} = 8.2$, *m*-Ph′), 132.55 (d, $^{2}J_{PC} = 17.6$, *o*-Ph), 134.07 (d, $^{2}J_{PC} = 21.1$, *o*-Ph′), 139.47 (d, $^{1}J_{PC} = 9.8$, *ipso*-Ph), 140.88 (d, $^{1}J_{PC} = 6.4$, *ipso*-Ph′), 184.44 [d, $^{2}J_{PC} = 29.3$ Hz, C(2)]; ^{31}P{^{1}H} NMR: δ −31.8 (s).

Table 1 Selected ^{1}H and ^{31}P{^{1}H} NMR data for **6**, **7**, **8**, **9** and **10** (δ in ppm) in $CDCl_3$

	Me	Me	Me	H^4	NMe$_2$	NCH$_2$	H$^{3\,a}$/Cp^b	^{31}P{^{1}H}
6	0.75	0.94	0.97	2.21 (t, 3.5 Hz)	2.86 (d, 2.4 Hz), 2.88 (d, 2.1 Hz)	3.92 (dd, 2.1, 13.5 Hz), 4.00 (d, 13.8 Hz)	—	26.76
7	0.77	0.91	0.91	2.96 (t, 3.9 Hz)	2.75 (d, 2.4 Hz), 2.87 (d, 2.7 Hz)	3.82 (dd, 3.0, 10.5 Hz), 4.44 (m)	4.24 (d, 13.3 Hz)	35.80, 35.79^d
8	0.67	1.03	1.13	4.44 (m)	—	—	—	31.07
9	0.80	0.94	0.99	3.01 (t, 4.5 Hz)	—	—	3.57 (m)	18.26
10^c	0.84	1.10	1.38	2.25 (br)	2.62, 2.83 (br)	n.f.	5.50	25.25

^{a} H^3 in **7** and **9**. ^{b} Cp in **10**. ^{c} At −40 °C. ^{d} In C_6D_6.

Synthesis of 3. Reaction of one equivalent of **1** in THF with 1.1 equivalent of *n*-BuLi at −78 °C was followed by the addition of 1 equivalent of [Cp_2TiCl_2] at −78 °C. The mixture was stirred overnight and the solvent removed under reduced pressure. Recrystallisation from toluene–*n*-hexane afforded **3** in 70% yield as a red solid. ^{1}H NMR: δ 0.70 (s, 3H, Me), 0.88 (s, 3H, Me), 1.08 (s, 3H, Me), 2.44 [m, 1H, H(4)], 6.46 (s, 10H, Cp), 7.26–7.32/7.50–7.54 (2 m, 10H, Ph); ^{13}C NMR: δ 11.17 [s, C(10)], 19.91/20.76 [2 s, C(8/9)], 27.60 [s, C(5)], 32.54 [s, C(6)], 52.43 [d, $^2J_{PC} = 6.0$, C(4)], 54.31 [s, C(7)], 60.45 [d, $^3J_{PC} = 5.8$, C(1)], 100.24 [d, $^1J_{PC} = 9.7$, C(3)], 117.40/117.91 (2 s, Cp), 127.32 (s, *p*-Ph), 128.11 (s, *p*-Ph′), 128.09 (d, $^3J_{PC} = 4.1$, *m*-Ph), 128.23 (d, $^3J_{PC} = 4.3$, *m*-Ph′), 132.29 (d, $^2J_{PC} = 17.5$, *o*-Ph), 134.01 (d, $^2J_{PC} = 20.1$, *o*-Ph′), 138.85 (d, $^1J_{PC} = 7.9$, *ipso*-Ph), 140.31 (d, $^1J_{PC} = 5.6$, *ipso*-Ph′), 189.70 [d, $^2J_{PC} = 27.4$ Hz, C(2)]; ^{31}P{^{1}H} NMR: δ −31.5 (s).

Selected data for 4. Satisfactory elemental analyses could not be obtained owing to the moisture sensitivity of the complex. ^{1}H NMR: δ 6.13 (s, 10H, Cp), 0.78 (s, 3H, Me), 1.02 (s, 3H, Me), 1.13 (s, 3H, Me), 2.35 [m, H(4)]; ^{31}P{^{1}H} NMR: δ −13.6 (d, $^1J_{P^{107}Ag} = 478.6$, $^1J_{P^{109}Ag} = 551.4$ Hz, with the expected magnetogyric ratios of ^{107}Ag and ^{109}Ag [$\gamma(^{107}Ag) : \gamma(^{109}Ag) = 0.87 : 1$]); FAB-MS *m*/*z* 998.8 (M^+).

Selected data for 5. Satisfactory elemental analyses could not be obtained owing to the moisture sensitivity of the complex. ^{1}H NMR: δ 6.14 (s, 5H, Cp), 0.80 (s, 3H, Me), 1.05 (s, 3H, Me), 1.20 (s, 3H, Me), 2.02 (s, MeCN), 2.52 [m, 1H, H(4)]; ^{31}P{^{1}H} NMR: δ −26.57 (s), −143 (sept, $^1J_{PF} = 714$ Hz, PF_6); FAB-MS: *m*/*z* 1195.1; does not correspond to the calculated value for $M^+ = 952.3$ but shows the expected Cu : Zr = 1 : 1 isotopic pattern.

Synthesis of 6. To a solution of **7** (0.26 g, 0.42 mmol) in THF (20 mL), potassium hydride (0.04 g, 1 mmol) was added at 0 °C. After the mixture was stirred overnight at room temperature, it was filtered and concentrated to 5 mL and then *n*-hexane (30 mL) added. At −30 °C, 0.15 g (0.26 mmol, 62%) of the beige product crystallized. Anal. Calc. for $C_{31}H_{36}NOPPd$: C, 64.64; H, 6.30. Found: C, 64.6; H, 6.1%. ^{13}C NMR: δ 9.62 [s, C(10)], 20.56/20.68 [2 s, C(8/9)], 28.56 [s, C(5)], 32.69 [s, C(6)], 49.16/49.54 (2 s, NMe$_2$), 55.74/55.91/56.78 [3 s, C(1/4/7)], 71.32 (s, NCH$_2$), 88.15 [d, $^1J_{PC} = 57.2$, C(3)], 122.11/123.41/125.39 (3 s, C_6H_4), 127.93 (d, $^2J_{PC} = 10.4$, *p*-Ph), 128.05 (d, $^2J_{PC} = 9.3$, *p*-Ph′), 129.35/129.52 (2 s, *o*-Ph/*o*-Ph′), 133.12 (d, $^3J_{PC} = 11.5$, *m*-P), 133.82 (d, $^3J_{PC} = 11.5$, *m*-Ph′), 134.41/135.10 (2 s, *ipso*-Ph/*ipso*-Ph′), 138.43 (d, $J_{PC} = 9.8$, C_6H_4), 147.53 (d, $J_{PC} = 6.3$, C_6H_4), 149.23 (s, C_6H_4), 200.23 [d, $^2J_{PC} = 19.3$ Hz, C(2)].

Synthesis of 7. To a solution of **1** (0.52 g, 1.55 mmol) in toluene (15 mL) [Pd(dmba)(μ-Cl)]$_2$ (0.43 g, 0.78 mmol) was added at room temperature. After the solution was stirred for 30 min, it was filtered and concentrated to 10 mL and then *n*-hexane (20 mL) added. At −30 °C 0.73 g (1.2 mmol, 77%) of the yellow product precipitated. Anal. Calc. for $C_{31}H_{37}ClNOPPd$: C, 60.79; H, 6.09. Found: C, 60.1; H, 6.70%. See NMR data in Table 1.

Synthesis of 8. To a solution of **9** (0.31 g, 0.37 mmol) in THF (20 mL) potassium hydride (0.04 g, 1.0 mmol) was added at 0 °C. After the mixture was stirred overnight at room temperature, it was filtered and concentrated to 5 mL and then *n*-hexane (30 mL) added. At −30 °C, 0.15 g (0.19 mmol, 52%) of the beige product crystallized. Anal. Calc. for $C_{44}H_{48}O_2P_2Pd$: C, 68.00; H, 6.22. Found: C, 67.5; H, 6.8%. See NMR data in Table 1.

Synthesis of 9. To a solution of **1** (0.89 g, 2.65 mmol) in THF (15 mL) [PdCl$_2$(SEt$_2$)$_2$] (0.47 g, 1.32 mmol) was added at room temperature. After the solution was stirred for 30 min, it was filtered and concentrated to 7 mL and then *n*-hexane (30 mL) added. At −30 °C, 0.93 g (1.09 mmol, 83%) of the orange product precipitated. Anal. Calc. for $C_{44}H_{50}Cl_2O_2P_2Pd$: C, 62.17; H, 5.93. Found: C, 61.4; H, 6.6%. See NMR data in Table 1.

Synthesis of 10. To a solution of **2** (0.40 g, 0.45 mmol) and LiBr (0.04 g, 0.45 mmol) in THF (30 mL) [Pd(dmba)(μ-Cl)]$_2$ (0.24 g, 0.44 mmol) was added at room temperature. After the solution was stirred for 1 h, it was filtered and concentrated to 8 mL and then *n*-pentane (20 mL) added. At −80 °C, 0.40 g of the beige product mixture precipitated.

X-Ray crystal structure determination of 2, 6 and 8·THF·H$_2$O

Crystal data for complex 2. A colourless crystal of **2** was coated with mineral oil, mounted on a glass fibre and transferred to the cold nitrogen stream (Bruker AXS Smart CCD System with Mo-Kα radiation ($\lambda = 0.71073$ Å) and graphite monochromator; Siemens LT-2 attachment). Crystal data: $C_{54}H_{58}O_2P_2Zr$, $M = 892.16$, monoclinic, space group $P2_1$, $a = 9.582(8)$, $b = 12.547(1)$, $c = 18.959(16)$ Å, $\beta = 97.67(1)$, $U = 2259(3)$ Å^3, $T = 143$ K, $Z = 2$, $D_c = 1.312$ g cm^{-3}, $\mu = 0.36$ mm^{-1}. A total of 24146 reflections ($\theta = 2.0$–$28.2°$) were collected (11141 independent reflections ($R_{int} = 0.066$)) and were used for structure solution (direct methods) and refinement (full-matrix least squares on F^2); $R1[I > 2\sigma(I)] = 0.0368$, $wR2$ (all data) = 0.0559. The hydrogen atoms were calculated and fixed in idealized positions. The absolute structure was determined with $x = -0.06(2)$. For all computations, the SHELXTL package (PC)[18] was used. Selected bond lengths and angles are given in Table 2.

Crystal data for complex 6. Colourless crystals from dichloromethane–*n*-hexane. A needle of **6** was coated with mineral oil, mounted on a glass fibre and transferred to the cold nitrogen stream (Bruker AXS Smart CCD System with Mo-Kα radiation ($\lambda = 0.71073$ Å) and graphite monochromator; Siemens LT-2 attachment). Crystal data: $C_{31}H_{36}NOPPd$, $M = 575.98$, monoclinic, space group $C2$, $a = 15.9544(15)$, $b = 31.8046(15)$, $c = 11.0466(12)$ Å, $\beta = 95.916(6)$, $U = 5575$ Å^3, $T = 173$ K, $Z = 8$, $D_c = 1.372$ g cm^{-3}, $\mu = 0.75$ mm^{-1}. A total of 18772 reflections ($\theta = 1.9$–$28.2°$) were collected (10447

Table 2 Selected bond lengths (Å) and angles (°) for **2** with estimated standard deviations in parentheses

Zr–O	1.995(2)	Zr–C(47)	2.520(3)
Zr–O′	2.009(2)	Zr–C(48)	2.537(3)
Zr–C(41)	2.522(3)	Zr–C(49)	2.552(3)
Zr–C(42)	2.525(3)	O–C(2)	1.327(3)
Zr–C(43)	2.518(3)	C(2)–C(3)	1.366(3)
Zr–C(44)	2.535(3)	P–C(3)	1.791(3)
Zr–C(45)	2.534(3)	O′–C(2)	1.333(3)
Zr–C(46)	2.497(3)	C(2′)–C(3′)	1.355(3)
		P–C(3′)	1.798(3)
O–Zr–O′	99.83(9)	Zr–O′–C(2′)	153.3(2)
Zr–O–C(2)	154.7(2)	O–C(2′)–C(3′)	130.3(2)
O–C(2)–C(3)	130.7(2)	C(2′)–C(3′)–P	125.4(2)
C(2)–C(3)–P	124.5(2)		

Table 3 Selected bond lengths (Å) and angles (°) for **6** with estimated standard deviations in parentheses

Pd–P	2.254(3)	Pd–C(11)	1.961(10)
Pd–O	2.122(6)	P–C(1)	1.744(9)
Pd–N	2.118(8)	O–C(2)	1.286(11)
P–Pd–O	86.06(18)	N–Pd–C(11)	82.5(4)
P–Pd–C(11)	99.6(3)	O–Pd–C(11)	173.8(3)
O–Pd–N	92.1(3)	N–Pd–P	177.36(18)

Table 4 Selected bond lengths (Å) and angles (°) for **8**·THF·H_2O with estimated standard deviations in parentheses

Pd–P(1)	2.260(2)	P(1)–C(13)	1.757(7)
Pd–P(2)	2.254(2)	C(13)–C(17)	1.355(9)
Pd–O(1)	2.097(4)	C(17)–O(1)	1.316(8)
Pd–O(2)	2.093(4)		
P(1)–Pd–O(1)	86.1(1)	O(2)–Pd–P(2)	85.9(1)
O(1)–Pd–O(2)	89.1(2)	P(2)–Pd–P(1)	98.84(6)

independent reflections ($R_{\text{int}} = 0.038$)) and were used for structure solution (direct methods) and refinement (full-matrix least squares on F^2); $R1[I > 2\sigma(I)] = 0.0383$, $wR2$ (all data) = 0.0775. The hydrogen atoms were calculated and fixed in idealized positions. The absolute structure was determined with $x = -0.06(3)$. For all computations, the SHELXTL package (PC)[18] was used. Selected bond lengths and angles are given in Table 3.

Crystal data for complex 8·THF·H_2O. Colourless crystals from THF–*n*-hexane. Kappa CCD diffractometer. Crystal data: $C_{44}H_{48}O_2P_2Pd\cdot C_4H_8O\cdot H_2O$, $M = 867.34$, monoclinic, space group $P2_1$, $a = 10.4840(2)$, $b = 34.0610(7)$, $c = 12.9620(2)$ Å, $\beta = 112.670(3)$, $U = 4271.1(3)$ Å^3, $T = 173$ K, $Z = 4$, $D_c = 1.35$ g cm^{-3}, $\mu = 0.552$ mm^{-1}, 4817 data with $I > 3\sigma(I)$, $R = 0.029$, $R_w = 0.035$. The absolute structure was determined with $x = -0.01(3)$. For all computations, the Nonius MoLEN package was used.[19] Selected bond lengths and angles are given in Table 4.

CCDC reference numbers 158617–158619.

See http://www.rsc.org/suppdata/dt/b0/b008227i/ for crystallographic data in CIF or other electronic format.

Acknowledgements

We are grateful to a referee for valuable comments, the Ministère de l'Enseignement Supérieur, de la Recherche et de la Technologie for financial support, the A. von Humboldt Foundation for a Feodor Lynen fellowship (to C. M.) and the CNRS for financial support and an associate research position (to C. M.) and the COST D12/0016/98 action of the European Commission (Brussels).

References

1 H. Brunner and W. Zettlmeier, *Handbook of Enantioselective Catalysis with Transition Metal Compounds*, VCH, Weinheim, 1993, vol. 2.

2 R. Noyori, *Asymmetric Catalysis in Organic Synthesis*, Wiley, New York, 1994.

3 W. A. Herrmann and B. Cornils, *Angew. Chem., Int. Ed. Engl.*, 1997, **36**, 1049.

4 A. Bader and E. Lindner, *Coord. Chem. Rev.*, 1991, **108**, 27; C. S. Slone, D. A. Weinberger and C. A. Mirkin, *Prog. Inorg. Chem.*, 1999, **48**, 233; P. Braunstein and F. Naud, *Angew. Chem., Int. Ed.*, 2001, **40**, 680.

5 See, for example: W. Keim, *Angew. Chem., Int. Ed. Engl.*, 1990, **29**, 235; W. Keim, *New J. Chem.*, 1994, **18**, 93; P. Braunstein, Y. Chauvin, S. Mercier, L. Saussine, A. DeCian and J. Fischer, *J. Chem. Soc., Chem. Commun.*, 1994, 2203; P. Braunstein, Y. Chauvin, J. Nähring, A. DeCian, J. Fischer, A. Tiripicchio and F. Ugozzoli, *Organometallics*, 1996, **15**, 5551.

6 R. M. Bullock and C. P. Casey, *Acc. Chem. Res.*, 1987, **20**, 167; G. S. Ferguson, P. T. Wolczanski, L. Párkányi and M. C. Zonnevylle, *Organometallics*, 1988, **7**, 1997; D. W. Stephan, *Coord. Chem. Rev.*, 1989, **95**, 41; A. M. Baranger and R. G. Bergman, *J. Am. Chem. Soc.*, 1994, **116**, 3822; P. Veya, C. Floriani, A. Chiesi-Villa and C. Guastini, *Organometallics*, 1994, **13**, 208; T. W. Graham, A. Llamazares, R. McDonald and M. Cowie, *Organometallics*, 1999, **18**, 3490; N. Wheatley and P. Kalck, *Chem. Rev.*, 1999, **99**, 3379; P. Braunstein and J. Rosé, in *Metal Clusters in Chemistry*, ed. P. Braunstein, L. A. Oro and P. R. Raithby, Wiley-VCH, Weinheim, 1999, vol. 2, p. 616, and references therein.

7 D. A. Knight, D. J. Cole-Hamilton and D. C. Cupertino, *J. Chem. Soc., Dalton Trans.*, 1990, 3051.

8 S. Berger, S. Braun and H.-O. Kalinowski, *NMR-Spektroskopie von Nichtmetallen*, Thieme Verlag, Stuttgart, 1993, vol. 3, p. 145.

9 M. D. Curtis, S. Thanedar and W. M. Butler, *Organometallics*, 1984, **3**, 1855.

10 (*a*) W. Spaether, K. Klass, G. Erker, F. Zippel and R. Froehlich, *Chem. Eur. J.*, 1998, **4**, 1411; (*b*) W. A. Howard, T. M. Trnka, M. Waters and G. Parkin, *J. Organomet. Chem.*, 1997, **528**, 95; (*c*) A. R. Siedle, R. A. Newmark, W. M. Lamanna and J. C. Huffman, *Organometallics*, 1993, **12**, 1491; (*d*) S. Gambarotta, S. Strologo, C. Floriani, A. Chiesi-Villa and C. Guastini, *Inorg. Chem.*, 1985, **24**, 654, and references therein.

11 F. H. Allen, O. Kennard, D. G. Watson, L. Brammer, A. G. Orpen and R. Taylor, *J. Chem. Soc., Perkin Trans. 2*, 1987, S1 and references therein.

12 S. Y. Lee and R. G. Bergman, *J. Am. Chem. Soc.*, 1996, **118**, 6396.

13 R. G. Pearson, *Inorg. Chem.*, 1973, **12**, 712; J. A. Davies and F. R. Hartley, *Chem. Rev.*, 1981, **81**, 79; J. Vicente, A. Arcas, D. Bautista and P. G. Jones, *Organometallics*, 1997, **16**, 2127.

14 (*a*) P. Braunstein, D. Matt, D. Nobel, S.-E. Bouaoud and D. Grandjean, *J. Organomet. Chem.*, 1986, **301**, 401; (*b*) P. Braunstein, D. Matt, Y. Dusausoy, J. Fischer, A. Mitschler and L. Ricard, *J. Am. Chem. Soc.*, 1981, **103**, 5115; (*c*) S.-E. Bouaoud, P. Braunstein, D. Grandjean, D. Matt and D. Nobel, *J. Chem. Soc., Chem. Commun.*, 1987, 488; (*d*) F. Balegroune, P. Braunstein, T. M. Gomes Carneiro, D. Grandjean and D. Matt, *J. Chem. Soc., Chem. Commun.*, 1989, 582.

15 C. Mattheis and P. Braunstein, *J. Organomet. Chem.*, 2001, **621**, 218.

16 (*a*) S.-E. Bouaoud, P. Braunstein, D. Grandjean, D. Matt and D. Nobel, *Inorg. Chem.*, 1986, **25**, 3765; (*b*) P. Braunstein, D. Matt, D. Nobel, F. Balegroune, S.-E. Bouaoud, D. Grandjean and J. Fischer, *J. Chem. Soc., Dalton Trans.*, 1988, 353; (*c*) P. Braunstein, L. Douce, J. Fischer, N. C. Craig, G. Goetz-Grandmont and D. Matt, *Inorg. Chim. Acta*, 1992, **194**, 151.

17 S. D. Perera and B. L. Shaw, *J. Organomet. Chem.*, 1991, **402**, 133.

18 G. M. Sheldrick, SHELXTL-PC, release 4.4, Siemens Analytical X-Ray Instruments, Madison, WI, 1992.

19 C. K. Fair, MoLEN, An Interactive Intelligent System for Crystal Structure Analysis, Nonius, Delft, Netherlands, 1990.